Laminar Burning Velocities of Atmospheric Coal Air Mixtures

Ho Young Park†, Yoon Hwa Park

KEPCO Research Institute, Korea Electric Power Corporation, 105 Munji-Ro Yuseong-Gu, Daejeon 30456, Korea
† bakhoy@kepco.co.kr

Abstract

The mechanism for laminar dust flame propagation can only be elucidated from a comprehensive mathematical model which incorporates conduction and radiation, as well as the chemical kinetics of particle devolatilization and gas phase and char reaction. The mathematical model for a flat, laminar, premixed coal-air flame is applied to the atmospheric coal-air mixtures studied by Smoot and co-workers, and comparisons are made with their measurements and predictions. Here the principal parameter for comparison is the laminar burning velocity. The studies of Smoot and co-workers are first reviewed and compared with those predicted by the present model. The effects of inlet temperature and devolatilization rate constants on the burning velocities are studied with the present model, and compared with their measurements and predictions. Their measured burning velocities are approximately predicted with the present model at relatively high coal concentrations, with a somewhat increased inlet temperature. From the comparisons, their model might over-estimate particle temperature and rates of devolatilization. This would enable coal-air mixtures to be burned without any form of preheat and would tend to increase their computed values of burning velocity.

Keywords : Burning velocity, devolatilization, coal combustion, char oxidation, coal air mixture

I. INTRODUCTION

Because of the complex phenomena involved in the combustion of pulverized coal in utility boilers, it is very difficult to isolate the key variables, or to create credible mathematical models of it. Recently, Lee and Choi [1] conducted the study for imaging quantification of the burning particles (coal being heated, volatile flame, and burning char) in terms of the changes of the apparent size, shape and intensity based on its luminosity. Their results for the fundamental combustion stages of single coal particles can reinforce the predictive modeling of coal combustion. Just as an understanding of turbulent gaseous flames depended on a prior knowledge of the corresponding laminar flames, understanding of laminar coal flames can contribute to deeper insights on the actual coal flames. There have been many works on the laminar coal air flames. The experimental works were somewhat specific to the individual experimental technique [2]-[12]. They include convective heating of the reactants from hot walls and preheated surface, radiative energy transfer, contact with other flame gases, increased inlet mixture temperature, and the addition of a small amount of gaseous fuel. Bradley et al [13] suggested that the burning of pulverized coal seems to be impossible without the aid of an external agency, and a variety of ways of achieving sustainable combustion are apparent. They also reviewed the burning velocities of coal-air flames at atmosphere. There was a wide range of burning velocities varying with the experimental conditions associated with the flame stabilizing methods.

The mechanism for laminar coal air flame propagation can be elucidated from a comprehensive mathematical model which incorporates, conduction, and radiation, as well as the chemical kinetics of particle devolatilization, gas phase and char reaction. The modelling studies were based principally upon particulate radiation, with the effects of conduction, devolatilization, gas-phase reaction, and diffusion added in steps [5][14][15]. Smoot et al. [9] performed modeling studies of the propagation of laminar premixed pulverized coal-air flames, which were stabilized below a smoothing screen [9]. Bradley et al. [13][16]-[18] have developed the mathematical model for a flat, laminar, premixed coal-air flame and checked by experimental works over a couple of decade.

Among the previous works, the detailed measurements to be comparable with the modeling results were made only by Smoot et al [8]. They measured the burning velocities of atmospheric, premixed coal air flames for a wide range of coal concentration (up to 1800 mg/L) with the downward burning using a flat flame burner with a smoothing screen. They also reported some profiles of temperature, gases and particulates behavior measured at 20 mm intervals throughout the flame. A model for a flame propagating in laminar, premixed coal-air mixture was formulated and compared with their measured burning velocities.

In the present study, the mathematical model for a flat, laminar, premixed coal-air flame used in the study of Bradley et al. [13] is applied to compare it with the atmospheric coal-air flames of Smoot et al [8]. Here the principal parameter for comparison is the laminar burning velocity. The experimental configuration employed by Smoot and co-workers [8] was similar to the configuration of the present model. For this reason, their experimental works are first reviewed in more detail and comparisons are made with the burning velocities of atmospheric laminar, flat, coal-air flames of both works.

II. MATHEMATICAL MODELLING OF LARMINAR PREMIXED COAL AIR FLAME

The mathematical model developed by Bradley et al. [13] is used for the present study. The model includes radiative heat transfer, detailed devolatilization scheme, reduced kinetics of gas phase and NOx, and detailed char and soot oxidation. The model

Manuscript received February 22, 2016, revised March 8, 2016, accepted March 15, 2016
ISSN 2465-8111(Print), 2466-0124(Online) DOI http://dx.doi.org/10.18770/KEPCO.2016.02.01.089

assumes a one-dimensional, infinite adiabatic flame with no heat losses to the burner. In the model, gas-phase combustion is modeled on the basis of a full chemical kinetic scheme, and gaseous transport fluxes are unaffected by the presence of particles, and diffusion of particles is neglected. The details of mathematical modeling and computational process are given in elsewhere [13][16]-[18]. Here only the brief description for the governing equations and laminar burning velocity is presented.

A. Governing equations and boundary condition

The governing equations are formulated in Eulerian form, except for the motion and energy balance of particles expressed in Lagrangian form. The time-dependent (t), one axial dimensional (y) conservation equations for two-phase system are as follows:

1) Global mass conservation equation

In this equation, M is the global axial mass flux, which is constant, and ρ_t the total density (both phases) of the mixture.

$$\frac{\partial \rho_t}{\partial t} + \frac{\partial M}{\partial y} = 0 \quad [\mathrm{kg}/m^3\mathrm{s}] \qquad (1)$$

2) Gaseous species, i, conservation equations

In this equation, the mass fraction *within the gas phase* of a gaseous species i is indicated by Y_{ig}. The fractional molar concentration, $\sigma_{ig}=Y_{ig}/m_i$, is introduced, where m_i is the molar mass. This equation is:

$$\rho_t\left(\frac{\partial(\sigma_{ig})}{\partial t}\right) + M\left(\frac{\partial(\theta\sigma_{ig})}{\partial y}\right) = -\frac{\partial(j_i/m_i)}{\partial} + R_i \quad (i = 1,2\cdots N)$$

$$[\mathrm{moles/m^3s}] \qquad (2)$$

where $\theta=\rho_g/\rho_t$, ρ_g is the gas density, j_i the diffusive mass flux of gaseous species i, and R_i its volumetric molar rate of formation. Rate constants for the gaseous species are given in Bradley et al [13].

3) Particulate species, k, conservation equations

For particulate species, Y_k indicates the mass fraction within both the solid and gaseous phase (*i.e. referred to both phases of the total mixture*) of the species, k. For the coal, k, includes carbon char, ash, primary volatiles and tar. For the tar, k, includes soot and secondary volatiles held in the tar, arising from primary devolatilization of the coal. The particulate species conservation equation is:

$$\rho_t\left(\frac{\partial Y_k}{\partial t}\right) + M\left(\frac{\partial Y_k}{\partial y}\right) = R_k m_k (k = 1\cdots K)$$

$$[\mathrm{kg/m^3s}] \qquad (3)$$

In this equation, there are no diffusive flux terms because diffusion in the solid phase is neglected. R_k [moles $\mathrm{m^{-3}s^{-1}}$] represents the general source term for the species.

4) Energy Equation

This equation includes both phases:

$$\rho_t\left(\frac{\partial h}{\partial t}\right) + M\left(\frac{\partial h}{\partial y}\right) = -\frac{\partial(q_c + q_d + q_r)}{\partial y} \qquad [\mathrm{W/m^3}] \qquad (4)$$

where h is the mass specific enthalpy of mixture. The energy fluxes q_c, q_d and q_r arise from gaseous thermal conduction, diffusion and radiation, respectively. Evaluations of gaseous specific heats, enthalpies, and transport properties associated with q_c and q_d are described in Dixon-Lewis [19]. The derivation and detailed explanation of the radiative energy flux, q_r, are given in detail in Bradley et al [17].

5) Equation of motion for a particle

The equation of motion for a reacting particle of velocity v_p is:

$$m_p \frac{dv_p}{dt_p} = F_N \qquad (5)$$

where m_p is the instantaneous mass of the particle, t_p the time and F_N the net force acting on the particle:

$$F_N = F_D + F_G + F_B \qquad (6)$$

where F_D is the aerodynamic drag force, F_G the gravitational force and F_B the buoyancy force.

6) Particle energy equation

The particle temperature, T_p, is obtained from the energy equation of the particle [17][18]:

$$q = h_c(T_p - T_g) + \sigma\varepsilon T_p^4 + \frac{1}{6}\frac{d(\rho_p c_p T_p d_p)}{dt_p} \qquad (7)$$

where q is the heat release rate per unit spherical external area. The three terms on the right represent the rate of heat loss by convection and radiation and the rate of accumulation of energy within the particle. The convective heat transfer coefficient is h_c, the particle emissivity ε, the Stefan-Boltzman radiation constant σ, the particle specific heat c_p, the particle diameter at position y d_p, and the particle density ρ_p.

7) Boundary condition

The conservation equations are solved subject to boundary conditions. These are

$$\begin{array}{lll} y_u = +\infty & \sigma_{ig} = \sigma_{ig,u} & \\ Y_k = Y_{k,u} & \mathrm{h} = h_u(T_u, \sigma_{ig,u}) & \\ \frac{\partial \sigma_{ig}}{\partial y} = 0 & \frac{\partial Y_k}{\partial y} = 0 & \frac{\partial h}{\partial y} = 0 \end{array} \qquad (8)$$

$$\begin{array}{lll} y_b = -\infty & & \\ \frac{\partial \sigma_{ig}}{\partial y} = 0 & \frac{\partial Y_k}{\partial y} = 0 & \frac{\partial h}{\partial y} = 0 \end{array} \qquad (9)$$

where the subscripts u and b refer to unburned and burned boundaries, respectively.

B. Laminar burning velocity

When the flame is propagating steadily, the burning velocity, S_u, is related to the mass flux, M, by [13][18] :

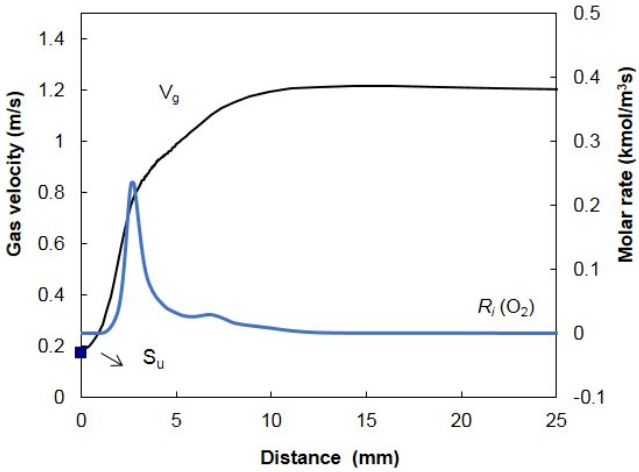

Fig. 1. Burning velocity, molar rate of O_2 and gas velocity

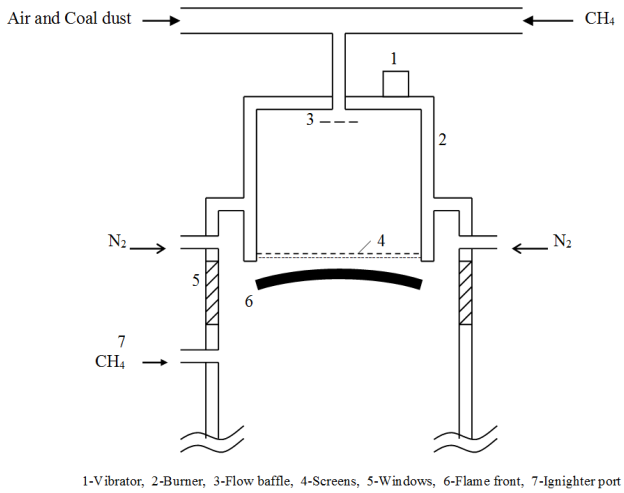

Fig. 2. Schematic drawing of burner system (Smoot et al., 1977a)

$$(M)=(M)_u=(M)_b=\rho_u S_u \tag{10}$$

where ρ_u is the unburned gas density, u is indicative of unburned and b of burned gas. The conservation equation for a species, i, in the steady state is expressed as :

$$t \to \infty : M\left(Y_{i,u} - Y_{i,b}\right) = \int_u^b \dot{m}_i dy \tag{11}$$

Here $\dot{m}_i$ is the volumetric mass rate of consumption of species i. The specific component "i" should normally be a rate controlling reactant and in the present model, i was chosen to be O_2.

The burning velocity, S_u, in the steady state, can be found by combining Eqs. (10) and (11), to give :

$$S_u \frac{1}{\rho_u} \frac{\int_u^b \dot{m}_i dy}{\left(Y_{i,b} - Y_{i,u}\right)} \quad [\text{m/s}] \tag{12}$$

The burning velocity found in this way converges rapi dly to the steady state value. The integral in Eq. (12) is e asily found from the source term of O_2 species equation (See Fig. 1).

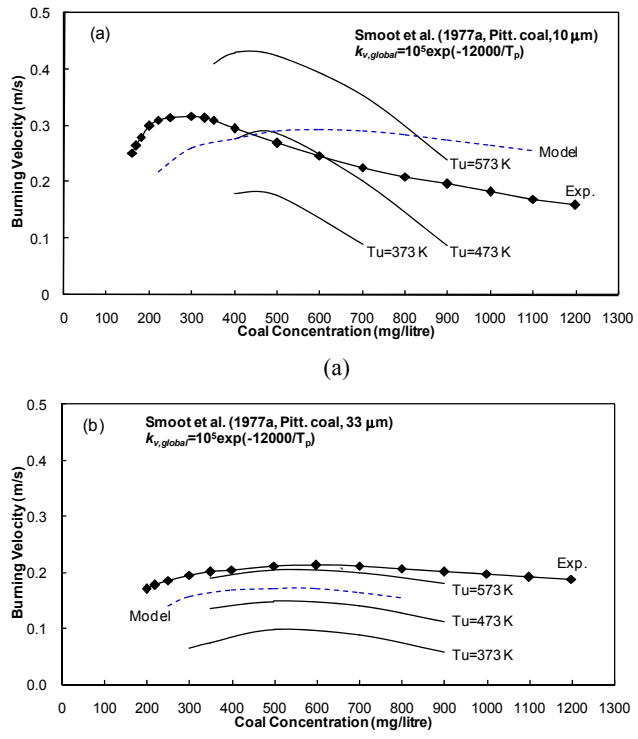

Fig. 3. Effects of inlet mixture temperature on burning velocity. $k_{v,global} = 10^5\exp(12000/T_p)$, (a) 10 μm, (b) 33 μm

III. REVIEW OF EXPERIMENTAL WORKS OF SMOOT AND COLLEAGUES

Smoot et al. [8] measured burning velocities for coal-air mixtures as a function of coal concentration, volatility, and particle size. They used a downward flowing, 10.16 cm diameter, flat flame burner at atmospheric pressure. A schematic diagram of their burner system is shown in Fig. 2.

Results showed that the finer size of coal particles gave a higher burning velocity on the lean side of the peak. The variations in volatile content had only a minor effect on the burning velocities. As a function of coal concentration, the burning velocity increased with coal concentration, reached a maximum, then decreased with further increases in concentration. For Pittsburgh coal (36.1 wt.% volatile on a dry basis), the burning velocities measured at 1 atm ranged from 0.14 to 0.22 m/s for 33 μm particles and from 0.16 to 0.33 m/s for 10 μm particles (See Fig. 3). It was also reported that the incoming combustible mixtures were heated to 573-673 K in the vicinity of the screens before reaching the flame front. These authors were of the view that preheating by the screen had no effect on the flame. Although they did not mention why the screen was preheated, it seems to be due to the necessary initial establishment of the flame with CH_4. There was no methane flow at the time of measurement.

In order to establish a coal-air flame, a relatively high flow rate of air and methane was firstly established and ignited by a

Table 1. Compositions of Pittsburgh coal (wt.%, dry)

	Char	CH_4	HCN	H_2	CO	CO_2	H_2O	Tar	Soot	Ash
Primary products	56.53	6.86	0.82	2.28	2.49	4.14	2.84	(17.93)		6.12
Secondary products		1.73	0.22	0.58	2.87				12.53	

Table 2. Rate constant of devolatilization used in the present model

Volatiles	Rate constants
Tar	$k_{v,\,tar} = 8.57\times10^{14}\exp(-27477/T_p)$
CH_4	$k_{v,CH4} = 2.51\times10^{5}\exp(-12028/T_p)$
HCN	$k_{v,HCN} = 1.2\times10^{12}\exp(-29188/T_p)$
H_2	$k_{v,H2} = 1.0\times10^{17}\exp(-45292/T_p)$
CO	$k_{v,CO} = 1.58\times10^{5}\exp(-8420/T_p)$
CO_2	$k_{v,CO2} = 1.26\times10^{5}\exp(-6014/T_p)$
H_2O	$k_{v,H2O} = 1.0\times10^{13}\exp(-17614/T_p)$

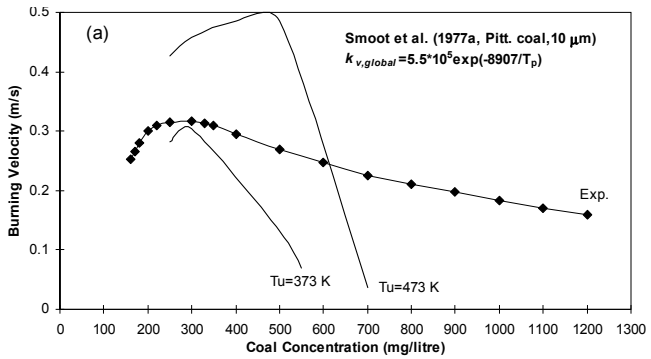

(a)

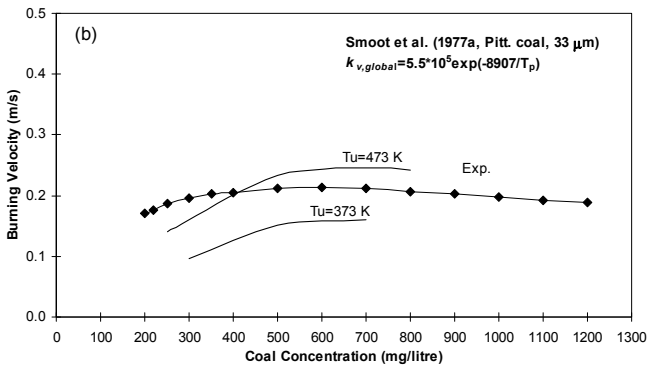

(b)

Fig. 4. Effects of inlet mixture temperature on burning velocity, $k_{v,global} = 5.5\times10^{5}\exp(8907/T_p)$. (a) 10 μm, (b) 33 μm

spark plug (not shown). Thereafter the feed rates of the solid, air, and methane were changed rapidly in small increments until the pre-selected ratios of feed rates were achieved and the flame was flat and laminar. In their experiments, it was difficult to establish the criteria for a free-standing, flat flame, because the flames often had a tendency to be cusp-shaped with the centre being closer to the screen. It was accepted as a free standing, flat flame whenever the centre of the flame was 0.1 inch away from the screen, even though the perimeter of the flame might be as much as 0.5 inch away from the screen. At this time, the gas flow rates were read directly from a flowmeter and, along with the total area of the screen, were used to calculate the burning velocity. It would seem that the burning velocity, S_u, was obtained from:

$$S_u = \frac{w}{\rho A} \ \text{[m/s]} \qquad (13)$$

where A is the screen area (m^2), w and ρ the mass flow rate (kg/s) and air density (kg/m^3), respectively.

IV. MEASURED BURNING VELOCITIES COMPARED WITH PREDICTIONS FROM THE PRESENT MODEL.

The experimental configuration employed by Smoot et al. [8] was that of a flat, laminar, premixed coal-air flame similar to the configuration of the present model. For this reason, their findings will be featured in rather more detail. The comparisons of burning velocities are made for Pittsburgh coal. Compositions of Pittsburgh coal are given in Table 1 and are used as input data for the present model. The values in Table 1 are obtained with the method of Merrick [20]. Particle diameters are 10 and 33 μm. With the present model, the speciated devolatilization rate constants, $k_{v,k}$, for each volatile species are employed, in addition to the two global rate constants, $10^5\exp(-12000/T_p)$ and $5.5\times10^5\exp(-8907/T_p)$. The values of $k_{v,k}$ are given in Table 2 [12].

In the experiments of Smoot et al. [8], the preheated screens seem to act as an extra energy source to sustain the pure coal-air flames, as previously discussed. They reported that incoming combustible mixtures were heated to 573-673 K in the vicinity of the screens, ahead of the flame. This does not represent the extent of any preheating from an extraneous source. Some reaction may be occurring to cause the temperature elevation and there can be radiative and convective heat transfer to the screens. The extent of any preheating of the mixture is likely to be determined by the energy gained by the screens from the combustion of the initial mixture containing methane. If the mixture would not burn without the addition of methane, it seems probable that its continuing combustion once the methane supply had been cut off must rest upon a degree of preheat, perhaps of the order of 100 K. The measurements made by these researchers suggest it could not have been great. Therefore, in the present model, this effect is modelled as an extra heat source that has preheated the inlet mixture. No combustion of coal-air mixtures was possible with this model unless the mixture was above the ambient temperature.

The effects on burning velocities of different modelled inlet mixture temperatures, T_u, with global devolatilization are shown in Fig. 3(a) for a particle diameter of 10 μm and Fig. 3(b) for 33 μm. Here $k_{v,global} = 10^5\exp(-12000/T_p)$, while in Fig. 4(a) and 4(b) $k_{v,global} = 5.5\times10^5\exp(-8907/T_p)$. Fig. 5(a) and 5(b) show predicted burning velocities with speciated volatiles, with the different rate constants, $k_{v,k}$, for each species. The experimental burning

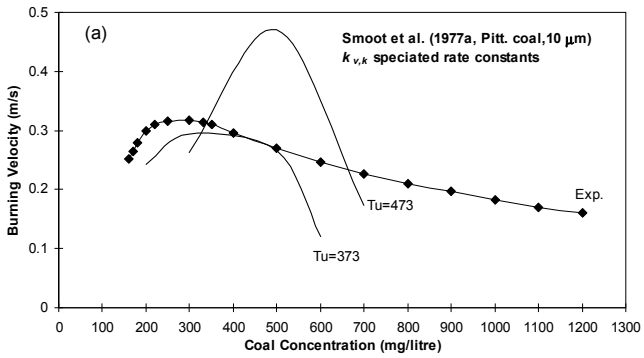

(a)

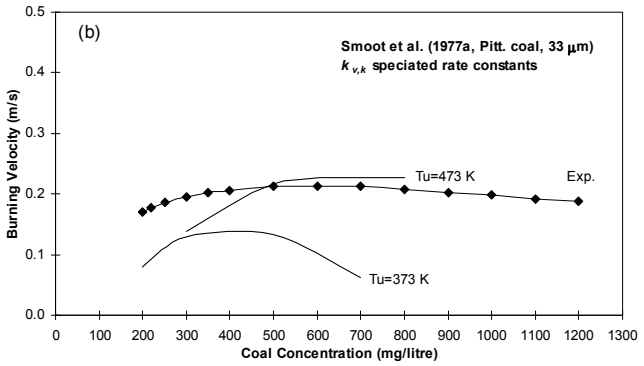

(b)

Fig. 5. Effects of inlet mixture temperature on burning velocity. speciated rate constants $k_{v,k}$. (a) 10 μm, (b) 33 μm

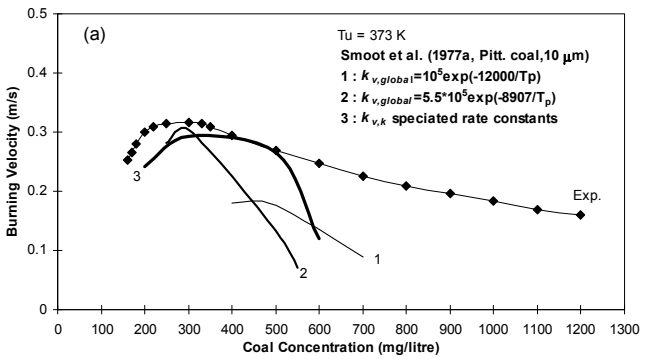

(a)

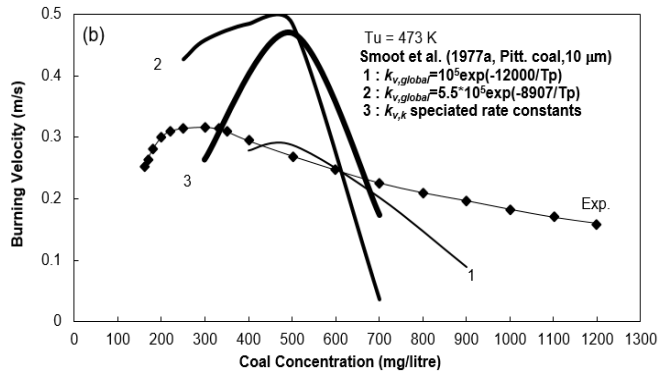

(b)

Fig. 6. Effects of rate constants on the burning velocities for 10 μm particles. (a) T_u = 373 K, (b) T_u = 473 K

velocities are those given by Smoot et al. [8], and the predicted ones of Smoot et al. [9] are also given in Fig. 3(a) and (b).

Fig. 3 through Fig. 5 show the predicted burning velocities to be very sensitive to the inlet mixture temperatures, T_u, especially for the 10 μm particle size. This is probably because the temperature of 10 μm particles is higher than that of the lager particles (33 μm). Because of the smaller thermal inertia the devolatilization is faster with the 10 μm particles. Also, the oxidation rate of the smaller char particles would be higher as a result of the higher volumetric reactive char surface area, at the same coal concentration.

In order to investigate the effects of different rate constants on the predicted burning velocity, the burning velocities predicted with the two values of global rate constants, $10^5\exp(-12000/T_p)$ and $5.5\times10^5\exp(-8907/T_p)$, and the speciated different rate constants, $k_{v,k}$, are again plotted with the experimental values. Fig. 6 shows the results for 10 μm particles at inlet mixture temperatures of 373 K and 473 K, respectively, and Fig. 7 shows the results for 33 μm particles at the same temperatures. At given inlet temperatures, the burning velocities predicted with the rate constant, $k_{v,global} = 10^5\exp(-12000/T_p)$, give relatively low values, compared to values predicted with other rate constants. The burning velocities predicted with the speciated rate constants, $k_{v,k}$, are very similar to those predicted with the global rate constant, $k_{v,global} = 5.5\times10^5\exp(-8907/T_p)$. Interpretation of these results is difficult because the extent of any preheating in the experiments of Smoot's group is unknown. In terms of these data, it might be argued from Fig. 6 (10 μm) that the better agreement between preheated and experimental values occurs at 373 K. From Fig. 7

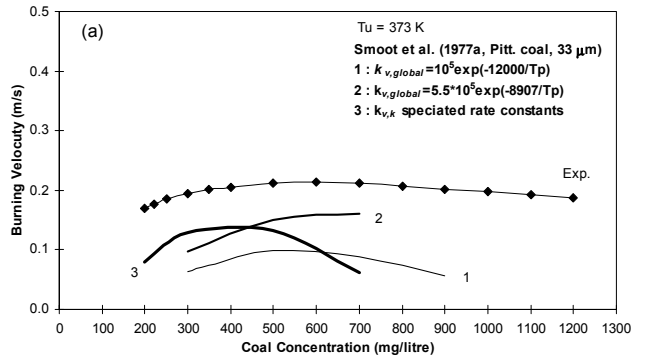

(a)

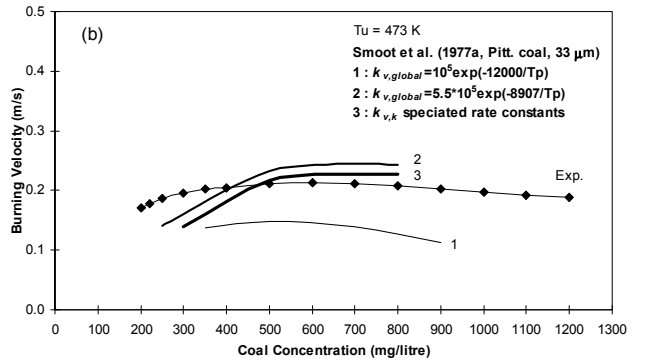

(b)

Fig. 7. Effects of rate constants on the burning velocities for 33 μm particle. (a) T_u = 373 K, (b) T_u = 473 K

Table 3. The present model and that of Smoot et al. [9]

	Smoot et al. [9]	Present Model
Gas phase species	10 species : H, O, OH, C_nH_m, O_2, H_2, CO, CO_2, H_2O, HO_2	24 species : H, O, OH, N_2, O_2, H_2, CO, CO_2, CH_4, H_2O, CH_3, CH_2O, CHO, HO_2, N, NO, CH_2, CH, HCN, CN, NCO, HNCO, NH, NH_2
Gas phase reaction mechanism	30 reactions (based on CH_4-air mechanism, Smoot et al., 1976) [15]	68 reactions (See Bradley et al., 2001)
Volatile species	C_nH_m, CO, H_2, N_2, OH	CH_4, HCN, H_2, CO, CO_2, H_2O, tar (soot, t-CH_4, t-HCN, t-H_2, t-CO)
Devolatilization rate constants	$k_{v,global} = 5.5\times10^5\exp(-8907/T_p)$	Can be varied
Volatile mixing	Diffusion of volatiles from the particle surface	Instant mixing with surrounding gases
Char reaction	Activated surface reaction and oxygen –diffusion controlled reaction	Surface reaction Molecular transfer
Char surface area factor (S)	1	Can be varied
Particle swelling	10 %	No
Ash	No	Yes
Coal particle heat capacity	0.3 cal/g K (constant)	Calculated from method of Merrick (1983) [20]

Table 4. Comparisons of the modelled results for a typical atmospheric coal-air flame (0.3 kg/m^3 coal concentration, 30 μm, and 1 atm)

Property Variable	Smoot model [9] T_u = 298 K	The present model $k_{v,global} = 5.5\times10^5\exp(-8907/T_p)$		The present model $k_{v,k}$ Speciated rate constans	
		T_u = 373 K	T_u = 473 K	T_u = 373 K	T_u = 473 K
Temp (K)					
Final gas	2078	1820	1866	1852	1914
Final particle	2080	1771	1811	1811	1863
Peak gas	2104	1860	1924	1878	1937
Peak particle	2164	1771	1811	1811	1863
Flame					
Burning velocity (m/s)	0.141	0.111	0.19	0.09	0.16
Thickness (mm)	9.9	10.2	10.8	10.3	10.8
% char reacted	0.3	35.3	44.3	35.4	43.9
% volatile reacted	99.4	99.9	99.9	99.9	99.9
Peak gaseous mole fraction in flame					
HC	0.0039/84	0.54×10^{-7}/38	0.60×10^{-7}/43	0.28×10^{-7}/57	0.19×10^{-7}/45
H_2O	0.1200/100	0.1364/100	0.1166/100	0.1173/100	0.1033/100
CO_2	0.1080/31	0.1190/35	0.1303/36	0.1333/37	0.1424/34
CO	0.0770/100	0.0548/100	0.0779/100	0.4336/100	0.0636/100
O	0.0028/28	0.0018/30	0.0032/32	0.0014/26	0.0026/32
OH	0.0054/31	0.0033/34	0.0038/36	0.2226/36	0.0031/37
H	0.0037/31	0.0019/36	0.0027/38	0.0015/38	0.0021/41
H_2	0.0210/100	0.0225/58	0.0302/59	0.0118/100	0.01520/64

(33 μm) the better agreement occurs at 473 K. It is probable that to burn the larger particles a greater degree of preheat was necessary. The observed increase in burning velocity for the smaller particle size is predicted by the model.

V. COMPARISON BETWEEN SMOOT MODEL AND THE PRESENT MODEL

Smoot et al. [9] developed the mathematical model of laminar premixed pulverized coal air flames and predicted the burning velocities. The predicted ones are given by label "Model" for 10 μm and 8-2 for 33 μm in Fig. 3. These were predicted with an inlet mixture temperature of 298 K and a global rate constant, $k_{v,global} = 5.5\times10^5\exp(-8907/T_p)$. The predicted burning velocities are given in Fig. 3. Without any preheat, this model was capable of burning pure coal-air mixtures and yielding burning velocities at high coal concentrations. Details of this model are compared with the present model and Table 3 gives the leading characteristics of both models.

The basic governing and auxiliary equations for the Smoot two phase system are similar to those in the present model. Both models assume an adiabatic flame, with no heat loss to the surroundings. The numerical methods of solution are similar. The basic assumptions for the particulate species are also very similar in both models. For example, in the Smoot model the initial coal particles are assumed to be composed of specified amounts of char (daf) and volatile matter, and no allowance is made for particle diffusion. However, the convective and diffusive flux terms in the gas phase equation seem to be simpler than those in the present model, as does the gas phase species reaction mechanism. The total amount of volatiles was 50 wt.%, but concentrations of each volatile were not reported. The Smoot char oxidation model is based on activated surface reaction, and the diffusion of reactant (oxygen) across the particle boundary layer.

For a typical atmospheric coal-air flame, concentration 0.3 kg/m^3, 30 μm Pittsburgh coal, Smoot et al. [9] have reported some values predicted by their model. These are summarised in Table 4, and compared with those of present model. For this comparison,

the devolatilization rate constants and char surface area factor in the present model are the same as in the Smoot model, that is, $k_{v,global} = 5.5\times10^5\exp(-8907/T_p)$. In addition, speciated rate constants, $k_{v,k}$, are used for the prediction.

Surprising aspects of the Smoot predictions are the high peak gas temperatures and the low percentage of reacted carbon. The former is as much as 800 K above the values of 1100-1300 K that were measured. For a similar coal-air flame, particle size 21 μm, concentration 380 mg/L, the measured carbon burn-out was about 22% and the measured devolatilization was 71%. On the other hand, the carbon burn-out and predicted peak gas temperature with the present model with $k_{v,global}$ are, respectively, 35.3% and 1860 K with T_u = 373 K, and 44.3% and 1924 K with T_u = 473 K. The present model with $k_{v,k}$ give, respectively, 35.4% and 1878 K with T_u = 373 K, and 43.9% and 1937 K with T_u = 473 K.

The Smoot model predicts that coal-air mixtures can be burned without any preheat or additional CH_4. This might be attributed to over-predicted particle temperatures and over-estimation of the concentration of volatiles. Since the peak particle temperature predicted was 2164 K, it might be that volatiles were modelled to evolve too readily. The proportion of volatiles (50 wt.%, daf) used in the Smoot model seems to be rather high.

Tar was not included as a volatile species in the Smoot model and it is not reported how particle temperatures were found. Therssen et al. [21] have measured coal particle temperatures in a flat flame, and found them to be 200 K lower than the gas temperature. It is concluded that the Smoot model might over-estimate particle temperature and rates of devolatilization. This would enable coal-air mixtures to be burned without any form of preheat and would tend to increase the computed values of burning velocity. In contrast to the Smoot model, the present model tends to predict lower burning velocities at the highest coal concentrations employed by Smoot and co-workers.

VI. CONCLUSION

The laminar burning velocity is a fundamental combustion parameter, notwithstanding the problems of measuring it accurately. In the present study, the mathematical model for laminar premixed coal air flames is applied to the atmospheric coal-air mixtures studied by Smoot et al. [8][9]. Detailed comparisons are made with the burning velocities of atmospheric laminar, flat, coal-air flames of Smoot and co-workers. With regard to the flat flame burner experiments of Smoot and co-workers, the measurements suggest that these flames were not adiabatic.

In the comparisons, the predicted burning velocities are very sensitive to the inlet mixture temperatures, especially for the smaller particle size. It might be due to the smaller thermal inertia increasing the devolatilization rate and the higher char oxidation rate for the smaller particles. The effects of devolatilization rate constants on the predicted burning velocity are tested with two global and speciated rate constants. The burning velocities predicted with the speciated rate constants are very similar to those predicted with the global rate constants used by Smoot and co-workers. The measured burning velocities deviated not only from the predictions of the present models, but also from the model employed by Smoot and colleagues. In the Smoot model, the particle temperature and devolatilization rate might be over-estimated so that the coal-air mixtures would be burned without any form of preheat and tend to increase the computed values of burning velocity. Compared to the Smoot model, the present model tends to predict lower burning velocities at the highest coal concentrations.

REFERENCES

[1] Lee H and Choi S. (2015). "An observation of combustion behavior of a single coal particle entrained into hot gas flow". *Combustion and Flame*, 162, 2610.

[2] Hattori H. (1956). "Flame propagation in pulverised coal-air mixtures". *Sixth Symposium (International) on Combustion*, The Combustion Institute, New York, 590.

[3] Ghosh B., Basu D. and Roy N.K. (1956). "Studies of pulverised coal flames". *Sixth Symposium (International) on Combustion*, Reinhold, New York, 595.

[4] Burgoyne J.H and Long V.D. (1958). "Some measurements of the burning velocity of coal-in-air suspensions". *Journal of The Institute of Fuel*, Paper No. 28.

[5] Marshall W.F., Palmer H.B. and Seery D.H. (1964). "Particle Size Effects and Flame Propagation Rate Control in Laminar Dust Flames". *J. Inst. Fuel*, 37, 342.

[6] Howard J.B. and Essenhigh R.H. (1967). "Mechanism of Solid-Particle Combustion with Simulation Gas-Phase Volatiles Combustion". *Eleventh Symposium (International) on Combustion*, The Combustion Institute, Pittsburgh, 399.

[7] Strehlow R.A., Savage L.D. and Sorensen S.C. (1974). "Coal dust combustion and supression". *Tenth AIAA/SAE Propulsion Conference*, San Diego.

[8] Smoot L.D., Horton M.D. and Goodson F.P. (1977a). "Characteristics of flat, laminar coal-dust flames". *Combustion and Flame*, 28, 187.

[9] Smoot L.D., Horton M.D. and Wiliams G.A. (1977b). "Propagation of laminar pulverised coal-air flames". *Sixteenth Symposium (International) on Combustion*, The Combustion Institute, Pittsburgh, 1455.

[10] Milne T.A. and Beachey J.E. (1977). "The Microstructure of pulverised coal-air flames. I. Stabilisation on small burners and direct sampling technique". *Combustion Science and Technology*, 16, 123.

[11] Slezak E.S., Fitch D.J., Krier H. and Buckius R.O. (1983). "Coal dust flame propagation in a laboratory flammability tube". *Combustion and Flame*, 54, 103.

[12] Bradley D., Dixon-Lewis G. and Habik S.E. (1989). "Lean flammability limits and laminar burning velocities of CH_4-Air-Graphite mixtures and fine coal dusts". *Combustion and Flame*, 77, 41.

[13] Bradley D., Lawes D., Park H.Y., and Usta N. (2006). "Modeling of laminar pulverized coal flames with speciated devolatilization and comparisons with experiments ". *Combustion and Flame*, 144, 190.

[14] Essenhigh R.H. and Csaba J. (1963). "The Thermal Radiation Theory for Plane Flame Propagation in Coal Dust Flames". *Ninth Symposium (International) on Combustion*, The Combustion Institute, Pittsburgh, 111.

[15] Smoot L.D., Hecker W.C. and Wiliiams G.A. (1976). "Predicting propagating methane-air flames". *Combustion and Flame*, 26, 323.

[16] Bradley D., Habik S.E. and El-Sherif S. (1991). "A Generilisation of Laminar Burning Velocities and Volumetric Heat Release Rates". *Combustion and Flame*, 87, 336.

[17] Bradley D., Chen Z., El-Sherif S., Habik S.E., John G. and Dixon-Lewis G. (1994). "Structure of Laminar Premixed Carbon-Methane-Air Flames and Ultra-Fine Coal Combustion". *Combustion and Flame*, 96, 80.

[18] Bradley D., Lawes D., Scott M.J. and Usta N. (2001). "The Structure of coal-air-CH_4 Laminar flames in a low-pressure burner: CARS measurements and modeling studies". *Combustion and Flame*, 124, 82.
[19] Dixon-Lewis G. (1984). "Computer Modelling of Combustion Reactions in Flowing Systems with Transport". *Chapter 2* in *Combustion Chemistry* edited by Gardiner W.C., Springer-Verlag, New York.
[20] Merrick D. (1983). "Mathematical Models of the Thermal Decomposition of Coal 1. The Evolution of Volatile Matter". *Fuel*, 62, 535.
[21] Therssen E., Gourichon L. and Delfosse L. "Devolatilization of coal particles in a flat flame-experimental and modeling study". *Combustion and Flame*, 103, 115.